Chapter 5
Spectroscopic Studies of Hydrocarbon, Air and Nitrogen Plasmas

> *"I think that a particle must have a separate reality independent of the measurements. That is an electron has spin, location and so forth even when it is not being measured. I like to think that the moon is there even if I am not looking at it."*
>
> *- Albert Einstein*

In the process of improving the understanding of the species present within various hydrocarbon and inert plasmas, optical spectroscopic measurements were made of six different plasma feedstocks: methane, ethylene, propylene, propane, nitrogen, and air. This analysis was the first step in evaluating these torch feedstocks as potential ignition sources. Plasmas are optically thin, losing energy at a much faster rate through emission than they gain by absorption. It is by using this property of plasma that measurements of the emitting species can be made. Hydrocarbon plasmas contain a high concentration of hydrogen atoms, which are well known to be good combustion enhancing radicals (Kimura et al., 1981; Takita et al., 2000). However, identifying other seemingly unimportant species, such as C_2, was important because they can participate in third-body chemical reactions from which combustion-enhancing radicals can be produced. Spectroscopic investigations of nitrogen and air feedstocks were conducted to provide reference spectrograms to aid in the identification of excited air species produced by interaction between the hydrocarbon plasmas and surrounding air. It should be noted that the spectroscopic analyses presented here were not used to deduce the concentration of the various species within the plasmas, but rather to provide an assessment of what types of species are present within such plasmas. In addition to these identification studies, two other studies were performed. One study was of the ratio of hydrogen and carbon lines within the plasma as a function of torch power; and the other was an analysis of molybdenum nitride peaks, which are indicative of electrode erosion.

Spectrographic analysis of each of the four hydrocarbon plasmas produced similar spectral 'signatures', demonstrating that each of the hydrocarbon plasmas contained the same basic species. Heavier hydrocarbons exhibited 'noisier' spectrograms, caused by multiple, weakly-emitting hydrocarbon fragments; but since these molecules radiate weakly, they were difficult to identify given the high emission intensity of surrounding atomic and diatomic species. The species identified from the spectrograms were placed into one of three categories: hydrocarbon fragments, hydrocarbon/air reactions, and excited air molecules. Identified hydrocarbon fragments include C_2, H_2, C, H, CH, and CH_2. Hydrocarbon plasma reactions with the surrounding air produced CN and NH. Finally, excited nitrogen and carbon dioxide molecules were detected, resulting from an energy exchange between the air and plasma. The contents of the air and nitrogen plasma showed evidence of a variety of oxygen and nitrogen band systems and were used to help identify various peaks within the hydrocarbon spectrograms that also appeared in the air and nitrogen spectrograms. The line ratio study demonstrated that changing the torch power could alter the relative concentration of species. Also, discovery of new molybdenum nitride peaks allowed the development of an anode erosion indicator to be developed. Consequently, through this study it was discovered that nitrogen was quite erosive to molybdenum anodes, which prompted a switch to copper anodes when nitrogen feedstocks were used.

5.1: Experimental Procedures

For these experiments, VTPT-3 was used with pure molybdenum anodes and 2% thoriated tungsten cathodes. The anodes had a 2.54 mm constrictor length and the traditional 0.178 mm gap setting was used. To ensure stable runs, higher input powers were necessary for the heavier hydrocarbon feedstocks. Also, the flowrate was set so that the internal torch pressure was 340 kPa for each test. Integration times for observing the various plasmas varied depending on the plasma intensity and were chosen to produce spectrograms near the upper end of the spectrometer dynamic range. To compensate for voltage fluctuations produced by the power supplies, spectral data were averaged over 35 voltage cycles, corresponding to 200 ms (i.e. if the integration time was 20 ms, 10 spectrograms would be taken and then averaged). Other operating conditions for the various tests are listed in Table 5.1.

Table 5.1: Torch Operating Conditions

	Current (A)	Voltage (V)	Power (W)	Integration Time (ms)
Methane	24.4	102	2490	40
Ethylene	24.4	129	3150	20
Propylene	41.0	110	4510	20
Propane	24.4	137	3340	20
Nitrogen	29.6	56.4	1670	150
Air	29.4	54.6	1610	150

5.2: Results and Discussion

The following discussion presents the results of the spectrographic studies of four hydrocarbon feedstocks, as well as air and nitrogen. Identification of atomic and molecular species was made by comparing observed spectral lines with compiled lists of known lines (Pearse, 1976; Gaydon, 1974; Tyte, 1964). All the species present within the methane plasma were observed in the other hydrocarbon plasmas as well, and so are discussed in detail only within the section involving the methane results. In addition, the species observed fall into three categories: hydrocarbon fragments, a result of hydrocarbon plasma and air interactions, and excited air molecules. These are discussed separately in their respective subsections. Two additional studies are also presented, one for the identification of molybdenum nitride peaks and another for the dependence of the ratio of hydrogen and C_2 line intensities on torch power.

5.2.1: Methane

The spectrogram used for identifying excited species within the methane plasma is shown in Figure 5.1. The major peaks are labeled, corresponding to the specie producing the spectral peak(s). Highly emissive species include atomic hydrogen and carbon, diatomic hydrogen and carbon, CN and CH. Close examination of the spectrogram showed the presence of excited CH_2, CO_2, N_2 and NH.

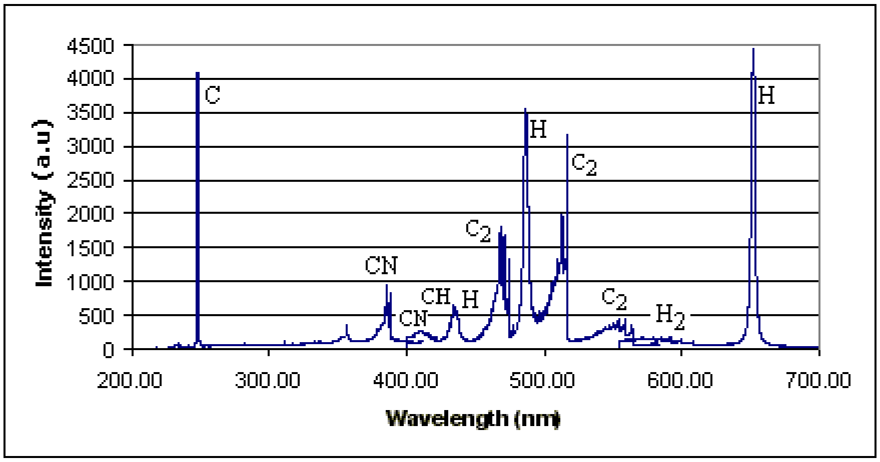

Figure 5.1: Methane Spectrogram

5.2.1.1: Hydrocarbon Fragments

The most identifiable features of the methane spectrogram are the presence of the strong atomic carbon line at 247.8 nm and the first three lines of the Balmer series for hydrogen at 656.3, 486.2, and 434.1 nm. Although weaker than the first three, the H_δ line is also present, but it is masked by the emission of excited CN molecules near 410 nm. The carbon line appears readily in hot flames with carbon-rich fuels and is usually quite intense. The Balmer lines for hydrogen are present in almost all hydrocarbon flames and are extremely bright, with the H_α line at 656.3 nm being the strongest. Both the atomic carbon and hydrogen lines produce singlets, indicative of monatomic species.

A number of diatomic species were detected as well, such as C_2, H_2, and CH. Several C_2 band systems were identified throughout the visible range. The strongest of these are the Swan band systems at 516.52, 563.55, 473.71 nm, with the 516.52 nm system, in the green, being the most intense. The occurrence of these bands is due to the $^3\Pi$—$^3\Pi$ transition. The Swan band systems are frequently encountered with sources containing carbon and all are degraded towards the violet. (When a band is described as being degraded in a certain direction, violet or red, it implies that the band intensity drops off more slowly in that direction, whereas it drops sharply in the opposite direction.) Two of the Swan band systems at 516.52 and 473.71 are shown in Figure 5.2, clearly exhibiting well-developed band heads and the characteristic violet degradation. A dim peak occurs at 468.02 nm and is caused by high-pressure interaction with surrounding gases (Pearse, 1976). In addition to the strong Swan band systems, a weaker C_2 band system is apparent near 410 nm, which is part of the Deslandres-D'Azumbuja system and is usually observed under high temperature conditions. The most intense head of this system appears at 385.2 nm, but in this case is masked by the strong CN Violet system and CH system near 388 nm.

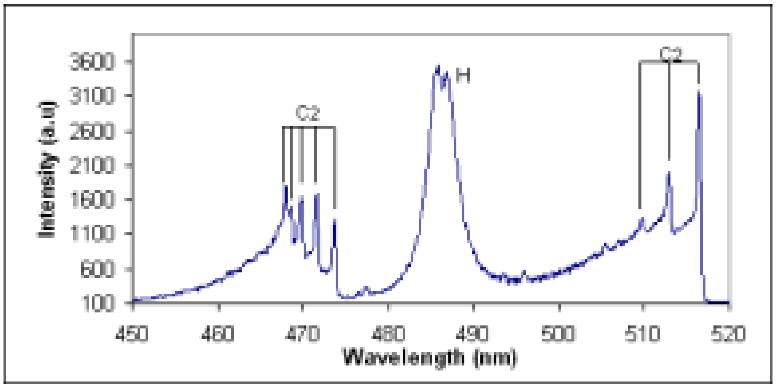

Figure 5.2: C_2 Swan Band Systems

An H_2 band structure was observed around 600 nm. Generally, the molecular hydrogen spectrum has few characteristic features, producing no groups of lines or heads resembling a typical band system. The H_2 molecule radiates quite weakly throughout the entire visible spectrum, but most intensely in the orange around 600 nm. The lack of other emitting species in this range was fortuitous, allowing the identification of excited H_2 to be made without the added difficulty of band superposition. The identification of hydrogen is usually made easier by the presence of the strong Balmer hydrogen lines, which are also present.

The three known systems of CH were observed near 430, 390 and 314 nm. CH bands are readily produced in electrical discharges where carbon and hydrogen are present. They exhibit an open rotational structure, characteristic of a diatomic hydride, and are due to the $A^2\Delta$—$X^2\Pi$ transition. The branches are double, indicating a molecule with an odd number of electrons, a rarity for an excited species. The 430 nm band system shown in Figure 5.3 is by far the brightest and is degraded towards the violet. The strong H_γ line partly obscures the CH band at 431.4 making the CH system appear less developed, but strong heads for this system were detected at 431.4, 432.3 and 438.5 nm. Interestingly, the strength of the head at 432.3 nm is highly variable and usually changes with the strength of the effective vibrational temperature. The remaining CH band systems at 390 and 314 nm both exhibit degradation towards the red. Strong heads were observed at 388.90 nm and 387.13 nm. The 314 nm band system is by far the weakest of the three, exhibiting only a few weak, closely packed heads. It is usually obscured by other species, in this case by excited N_2.

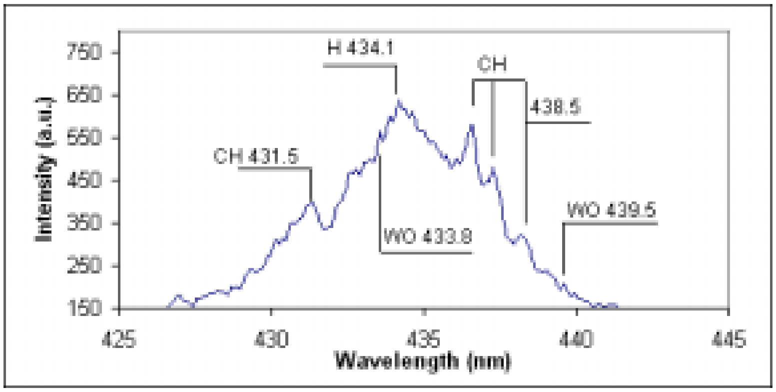

Figure 5.3: CH Bands and H_γ Line near 430 nm

In addition to the aforementioned atomic and diatomic species, it was expected that emission spectra of CH_3 would be present; but they were not. The strongest bands are in the vacuum ultraviolet near 150 nm, well outside the visible range. Bands for CH_3 do occur in the ultraviolet near 216 nm, but are relatively weak and were not detected in this study. Band systems due to polyatomic molecules are less common in the visible region than those due to diatomic molecules. In addition, methyl radical peaks are usually produced best in absorption using flash photolysis, or low-pressure flames of methane, and therefore would not necessarily be produced in emission spectra for methane plasma. However, CH_2 peaks near 537.5 nm were detected, indicating the presence of triatomic species within the plasma jet.

5.2.1.2: Hydrocarbon-Air Molecules

Interactions between excited hydrocarbon species and surrounding air molecules were detected by the presence of CN and NH. Two band systems for CN were observed in the methane spectrogram, the Violet and LeBlanc systems. These systems are common in hot flames as an impurity, and in this case are caused by the interaction of the methane plasma with the surrounding air. The Violet band system, caused by the $B^2\Sigma$—

$X^2\Sigma$ transition, radiates strongly from 350 to 460 nm with the most identifiable band heads at 421.60, 388.34 and 359.04 nm. The heads in this system are degraded towards the violet and are evenly spaced. An example of the 421.60 band system appears in Figure 5.4a. Here, the CN band head at 421.60 nm appears to be the least intense peak, when in actuality the Deslandres-D'Azumbuja C_2 system at 410 nm merges with the weaker CN peaks making them appear stronger than the band head. This phenomenon is known as band superposition and occurs frequently with samples containing closely radiating species. The most intense of the three Violet band systems is the system at 388.34 nm, but it is usually masked by the strong CH band near 390.0 nm unless it radiates strongly. In this case, the emission intensity of the 388.34 nm CN band system is sufficient to be observed, even through the strong CH band system, as shown in Figure 5.4b. This demonstrates another example of band superposition, one more commonly observed in hydrocarbon flames. The third, and least intense of the CN Violet band systems at 359 nm, is usually clear from any overlapping and often appears in the spectra of hot flames interacting with nitrogen. However, this band system was absent in the methane spectrogram, masked by the excited nitrogen spectra near 358 nm. As a final note, the LeBlanc system of CN, although much weaker than the Violet system, had observable peaks at 423.90 and 429.24 nm.

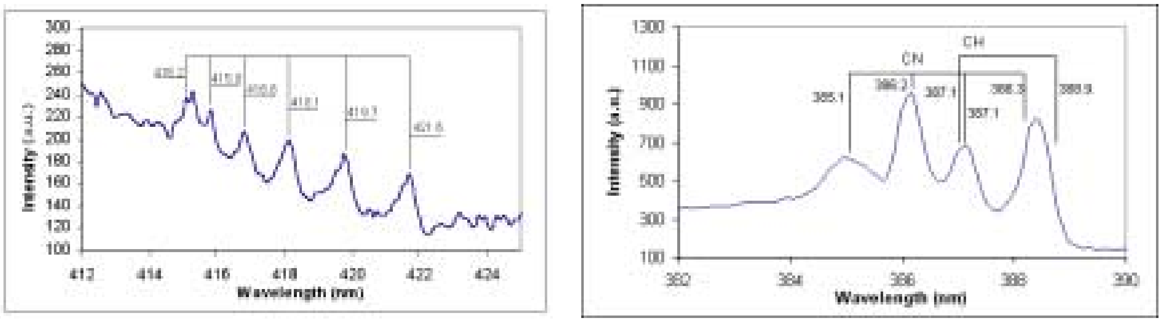

(a) CN Violet Band System at 421.60 nm (b) Merging of CN Violet and CH bands near 390 nm

Figure 5.4: CN Violet Band Systems

NH bands, which usually appear weakly in hot flames with air as well as low-pressure arcs, were also observed in the methane spectrogram. Diffuse heads were detected at 336.0 and 337.0 nm, with a well-defined head at 338.3 nm, as shown in Figure 5.5. These bands are part of the 336.0 nm system and are produced by the $A^3\Pi$—

$X^3\Sigma^-$ transition. The band structure for NH in this region is not clearly degraded towards either the red or violet, and is rather weak.

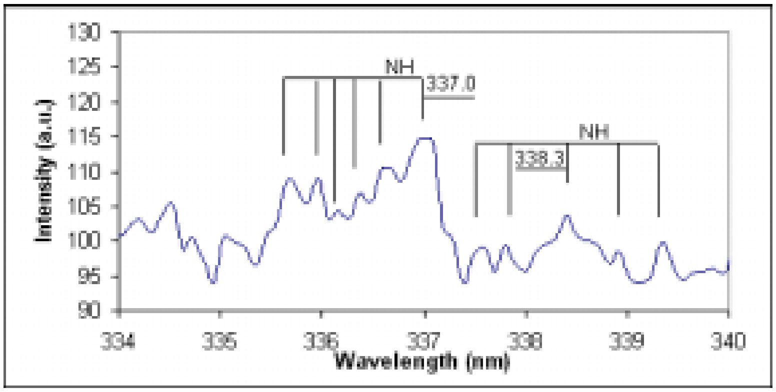

Figure 5.5: NH Bandheads at 336 nm

5.2.1.3: Excited Air Molecules

In addition to the hydrocarbon fragments and products of air/plasma reactions mentioned above, excited CO_2 and N_2 molecules were also detected in the methane plasma. Faint CO_2 bands were observed from 426 to 441 nm, associated with the Carbon Monoxide Flame Bands of CO_2, and produced by the transition $^1B_2$—$X^1\Sigma^+$. These bands are generally observed in the flames of carbon monoxide burning in air, but can also be produced by a heavy-current discharge through carbon dioxide.

Bands from the Second Positive System of N_2 were found from 310 to 360 nm, with the strongest head at 357.69 nm. Shown in Figure 5.6, identification of this band system proved troublesome at first, until analysis of a pure nitrogen plasma spectrogram showed the same system, considerably narrowing the field of possible emitters. The Second Positive System of Nitrogen is most easily produced with a discharge through air. The heads are usually degraded towards shorter wavelengths and are produced by the $C^3\Pi_u$—$B^3\Pi_g$ transition. The head at 333.90 nm is often fairly weak; but with discharges through air, the strength of the head can be increased considerably, as is noticeable in this case.

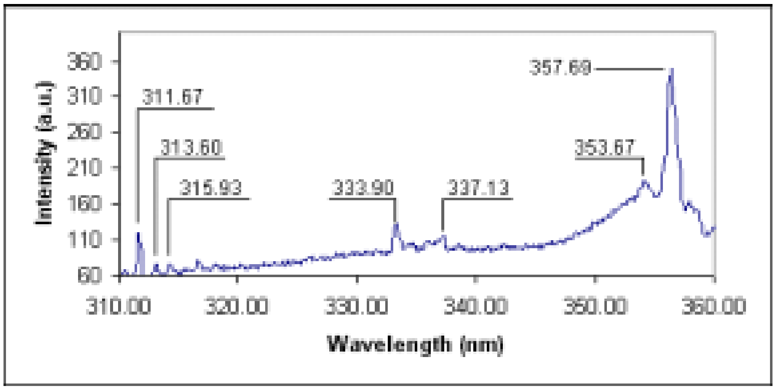

Figure 5.6: N_2 Second Positive System

5.2.2: Ethylene

The spectrogram of ethylene plasma, shown in Figure 5.7, exhibited little difference from the methane spectrogram taken under similar conditions. All of the species that appear in the methane spectrogram appear here in the ethylene spectrogram, with no identifiable new ones. Even the line ratios appear similar, except for the H_β line, which appears slightly weaker.

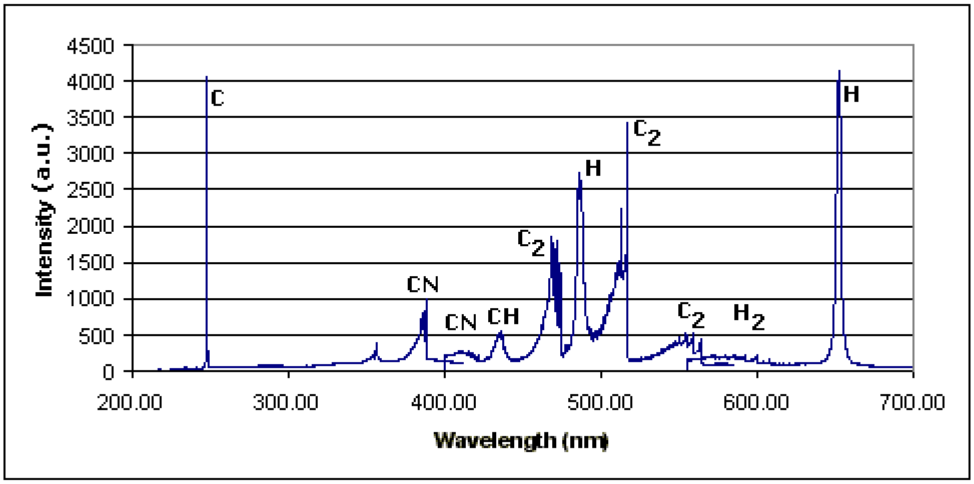

Figure 5.7: Spectrogram of Ethylene Plasma

5.2.3: Propane and Propylene

Propane and propylene plasmas produced similar spectrograms to the earlier hydrocarbons, although the line ratios are different, as shown in Figure 5.8. In addition, it seems there is a large source of broadband emission centering around 550 nm, which is nearly absent in the methane and ethylene spectrograms. Previously unidentified peaks of molybdenum nitride were discovered at 524 and 536 nm. This is discussed in Section

5.2.6. In addition, more spectral peaks from excited nitrogen were observed throughout the visible range, with the strongest occurring between 240 and 350 nm.

One interesting phenomenon that occurred when testing the different fuels was the observable brightness of the plasma jet itself. It was found that as the number of carbon atoms in the torch feedstock increased, the brightness of the plasma jet also increased. The methane plasma jet was dim relative to the jets of ethylene, propylene, and propane. The propylene plasma was by far the brightest of the four, with an intensity greatly exceeding that of any other feedstock tested. Gaydon (1974) notes that fuels with higher carbon contents produce the most luminous inner cones for flames, and the observations presented here for hydrocarbon plasmas agree with his findings.

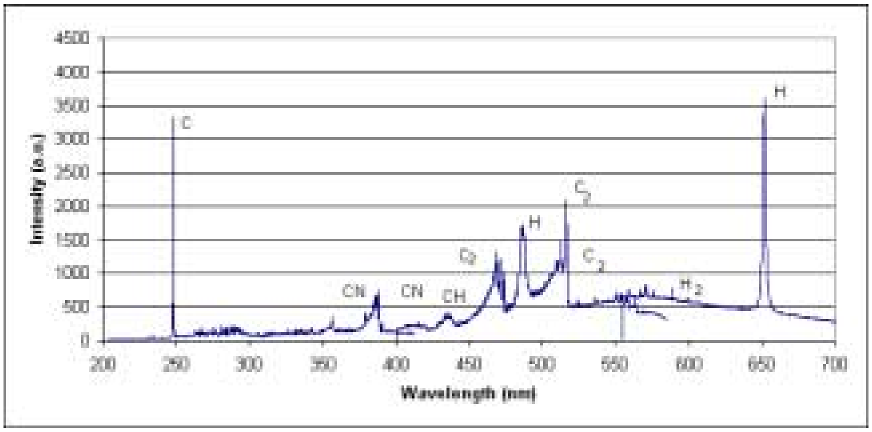

(a) Propane Plasma

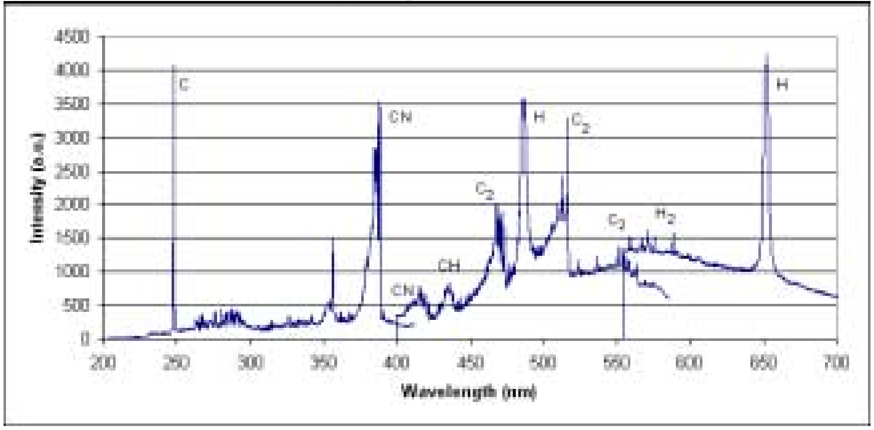

(b) Propylene Plasma

Figure 5.8: Spectrograms of Propane and Propylene Plasmas

5.2.4: Nitrogen and Air

Nitrogen and air plasma spectrograms were observed to contain a large number of peaks and to cause a lot of superposition, sometimes making identification of various band heads difficult. A large number of band systems attributed to both nitrogen and oxygen species exist, which radiate strongly over the entire visible spectrum. The most intense of these occur between 250 and 400 nm.

Spectral analysis of nitrogen plasma showed the presence of the First, Second, Fourth, and Fifth Positive Systems, and the Vegard-Kaplan Bands of nitrogen. The ranges for each of these systems are shown in Figure 5.9. All of these band systems appear in emission and are readily produced in a discharge. The Second Positive System is more easily obtained with a nitrogen discharge through air, as shown here, because the oxygen seems to prefer the Second Positive System rather than the usually stronger First Positive System. Peaks from the First Positive System are shown in Figure 5.10, along with some peaks from the First Negative System for N_2^+. In addition to excited oxygen and nitrogen species, evidence for NO was detected at 380 nm as well as other peaks from the NO_β System. In addition, strong emission bands from NO_2 were found from 430 to 480 nm.

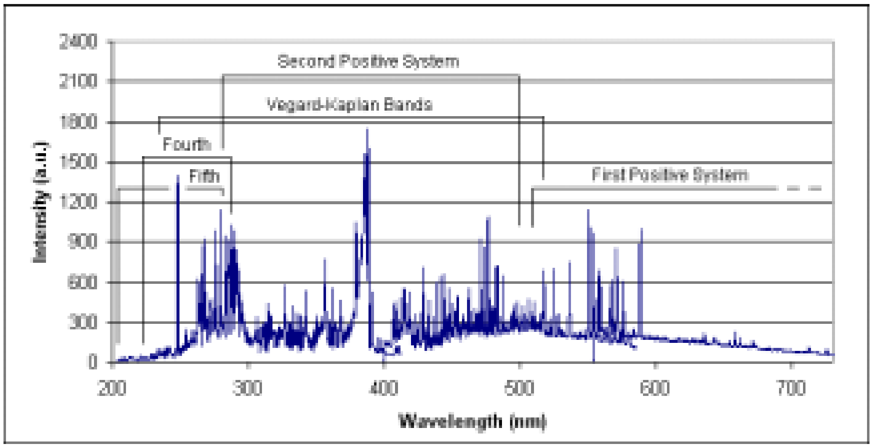

Figure 5.9: Spectrogram of Nitrogen Plasma

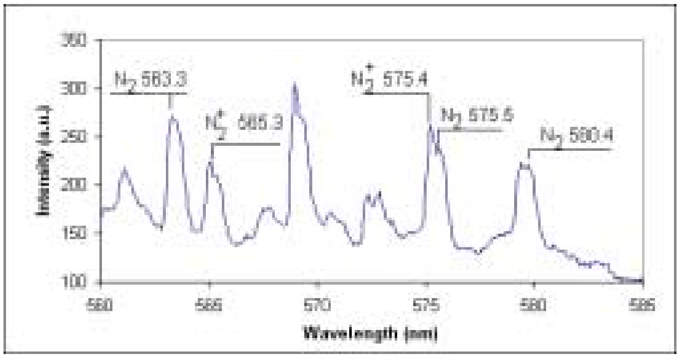

Figure 5.10: Neutral and Charged Nitrogen Peaks

The air plasma spectrogram shown in Figure 5.11 is quite similar to the nitrogen, with only a few minor differences. The well-known emission band systems of oxygen are labeled as a convenient reference. The spectrogram is presented on a reduced scale to show some detail in areas of interest. Often, the neutral oxygen molecule does not show an emission spectrum except under certain conditions; but strong peaks from the molecular oxygen Schumann-Runge System were identified at 367.1, 351.7, 337.0 and 287.0 nm. As before, the strong presences of the Second, Fourth and Fifth Positive Systems of nitrogen are evident. The First Positive System was not in evidence due to the presence of excited oxygen. Another interesting difference between the air and nitrogen plasma spectrograms occurs near 385 nm. Figure 5.12 shows a detailed view of this spectral region for both air and nitrogen plasmas. There are three major peaks present in the air spectrogram at 379, 386 and 391 nm, which are all present within the nitrogen spectrogram as well. However, a definite source of broadband emission exists in the nitrogen spectrogram, which is completely absent with the air. The source of this emission is not known, but may provide a topic for future research.

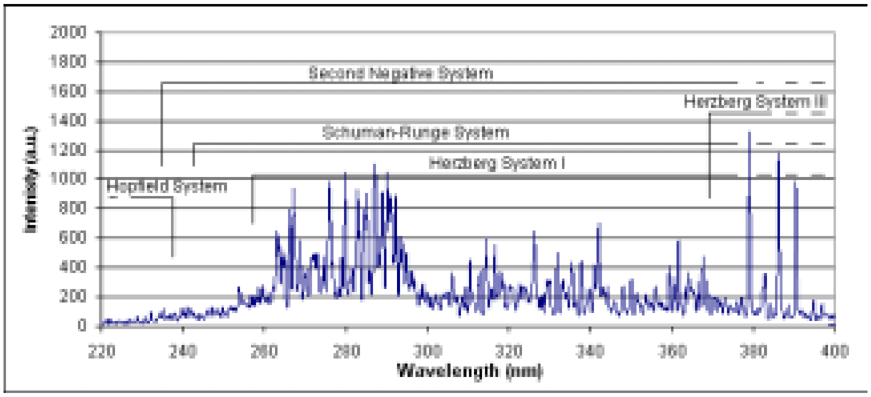

Figure 5.11: Spectrogram of Air Plasma

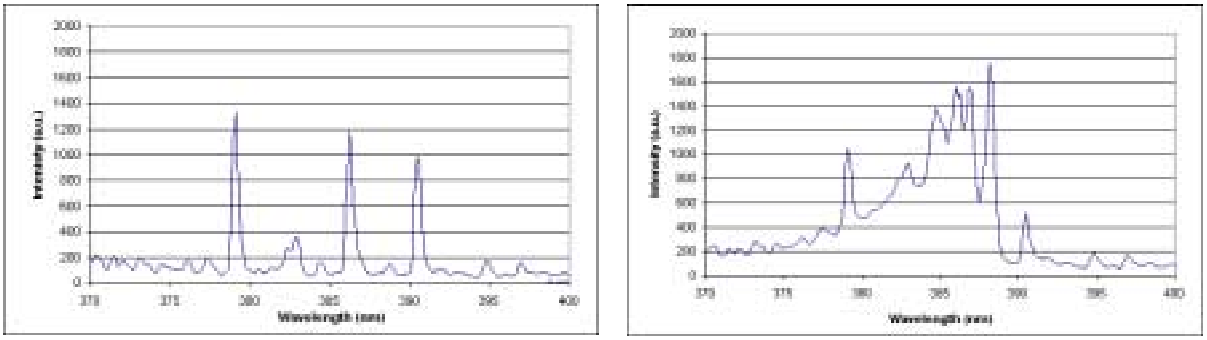

(a) Air Spectrogram (b) Nitrogen Spectrogram

Figure 5.12: A Comparison of Air and Nitrogen Plasma Spectra

5.2.5: Discovery and Analysis of Molybdenum Nitride

An extremely interesting discovery from the propylene and propane spectrograms was the presence of previously unobserved spectral lines at 524.02 nm and 536.16 nm. Samples of the six spectra from the six different feedstocks in this region are shown in Figure 5.13. The maxima of these peaks may be slightly shifted towards the red due to the nearby C_2 Swan bands at 550 nm. Two smaller heads can be seen at 526.01 nm and 528.25 nm, indicating that this band system is degraded towards the red. In addition, the nitrogen and propylene spectrograms show the main heads as singlets; whereas in the air spectrogram, and even more so in the propane, the heads are clearly closely packed triplets. A listing of these peaks and their appearance is recorded in Table 5.2. The presence of multiple heads with a triplet structure indicates at the bare minimum a diatomic molecule, but perhaps a heavier polyatomic molecule. Consequently, the flat peak near 538 nm in the hydrocarbon spectrograms is emission by the methylene radical, CH_2, which produces a peak at 537.5 nm; but in this case it is shifted slightly towards the red because of the nearby emission of C_2 at 550 nm.

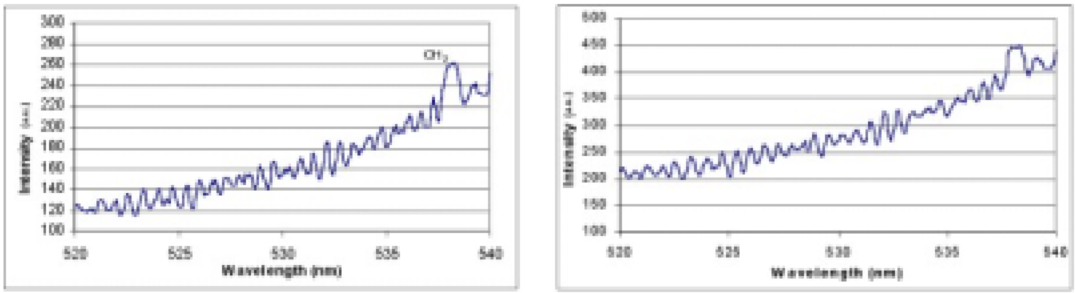

Methane Ethylene

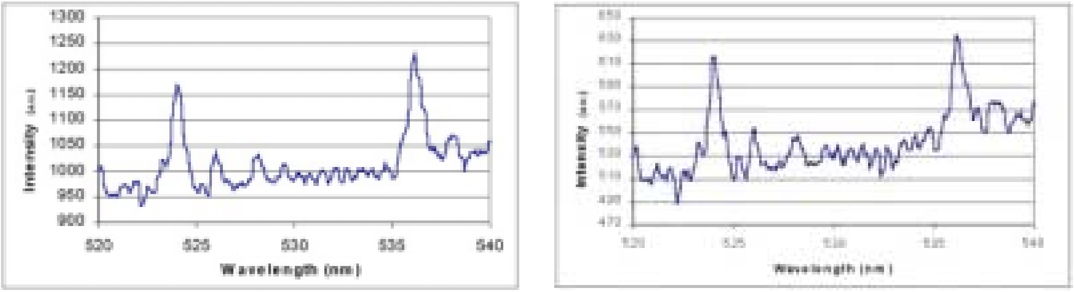

Propylene Propane

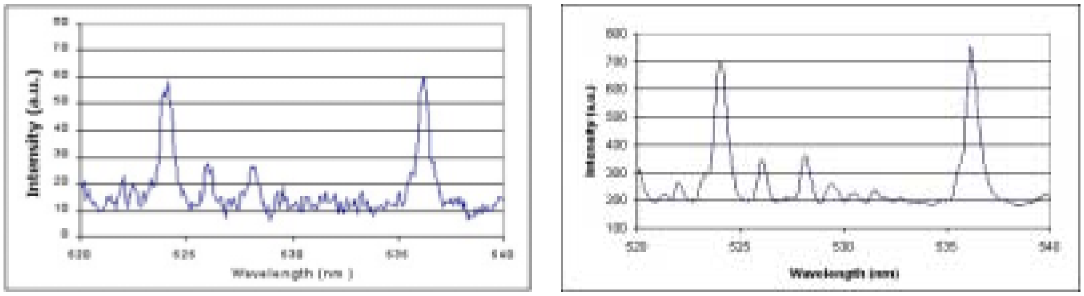

Air Nitrogen

Figure 5.13: Molybdenum Nitride Peaks at 524.02 and 536.16 nm

Table 5.2: Spectral Peak Characteristics in the 520-540 nm Range

Wavelength (nm)	Intensity (10=max)	Appearance	Degradation
524.11	9	Triplet	None
526.01	4	Doublet	None
528.25	5	Doublet	None
536.16	10	Triplet	None

At first these peaks were thought to be emission from a heavier hydrocarbon fragment, explaining the absence of the peaks in the methane and ethylene spectrograms. However, the same peaks, exhibiting the same proportions, were also observed in the nitrogen and air plasmas, thus limiting the chemical composition of the emitter to a molecule containing a combination of nitrogen, oxygen or molybdenum. Research of known nitrogen, oxygen and N_xO_y systems demonstrated the emitter could be attributed to none of these. The only matching peaks in any of these systems occur in the First Negative Systems of both O_2^+ and N_2^+, which have strong peaks near 524 nm, but are degraded towards the violet; whereas for this band, the peaks are degraded towards the red. In addition, the other known peaks in the O_2^+ and N_2^+ systems did not appear in the other regions of the spectrogram and neither system had peaks matching the 536.16 nm peak.

Having effectively ruled out the emitter as containing solely nitrogen or oxygen, the only plausible explanation is that the emitter must contain molybdenum. Repeating the experiments with a copper anode confirmed this theory. As shown in Figure 5.14, the strong peaks at 524 and 536 nm are completely absent when a copper anode is substituted for molybdenum. This proves the emitter must be either Mo_xO or Mo_xN. Tungsten nitrides and oxides are discounted, since very little tungsten from the cathode is consumed during testing. In addition, MoO is not known to emit in the yellow, where these peaks are present, but more readily emits in the red and near infrared. From the long list of possible emitters, MoN is left as the most plausible candidate.

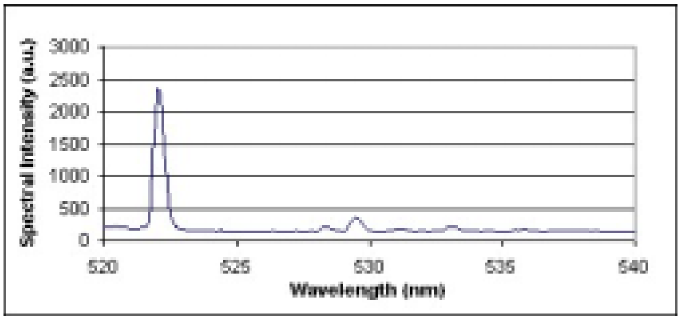

Power: 1500 W
Feedstock: N_2
Scope: 1-mm diameter
Position: 1 mm above torch exit
Integration Time: 400 ms
Cross flow: M=2.4
Anode: Copper

(a) Spectrogram of N_2 Plasma with Copper Anode

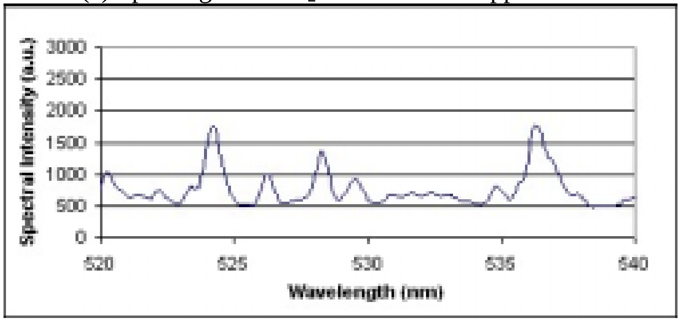

Power: 1420 W

Note: The strong peak near 522 nm in Figure 5.10a, caused by excited nitrogen, appears much less intense in Figure 5.10b. As discussed earlier, the presence of metallic particles in a flame or plasma can affect the intensity of spectral lines.

(b) Spectrogram of N_2 Plasma with Molybdenum Anode

Figure 5.14: Comparison of N_2 Plasma Spectra with Copper and Molybdenum Anodes

Now that the list of possible emitters has been considerably shortened, the presence of the peaks in propylene, propane, air and nitrogen spectrograms, and their absence in the methane and ethylene spectrograms, is much more easily explained. The presence or absence of these peaks is linked to the rate of anode erosion, which is a function of the feedstock gas used. It is well known from previous work that heavier hydrocarbons, such as propylene, produce far more electrode erosion than lighter hydrocarbons, such as methane and ethylene (Gallimore, 1998). In addition, during the work, it was discovered that air and nitrogen plasmas are extremely erosive to molybdenum. Numerous studies involving nitrogen as a torch feedstock were performed; but none of these have used molybdenum anodes, explaining the lack of publication on this phenomenon (Hardy, 1985; Auwter-Kurtz et. al., 1997; Shuzenji et. al. 2000; Takita et. al. 2000).

An example of anode erosion caused by active nitrogen is shown in Figure 5.15a, where flow is from left to right. The presence of a dull silvery substance on the anode surface indicates a compound is being formed, which is a product of the nitrogen plasma and the molybdenum anode. The anode constrictor has been severely eroded by the arc, which formed a large cavity extending several millimeters downstream. The area immediately downstream of the constrictor is covered with a fine powdery substance, believed to be molybdenum nitride. A sample of the powder was examined under a microscope at 1000X magnification and a definite crystal structure was observed, as shown in Figure 5.15b. Although identification of the crystal structure could not be made through the microscope, the cross-sectional area of each crystal is about one square micrometer. These crystals clumped together to form the larger shapes noticeable throughout the photo.

The case for molybdenum nitride, MoN, seems to be a rational one, since nitrogen is erosive to molybdenum. Also, the spectrographic measurements identify the chemical composition of the emitter. Howard and Conway (1965) performed similar experimental work in the 1960s with molybdenum electrodes in air, and also with plasma jets, to identify peaks of Mo_xO and Mo_xN. They discovered MoN peaks from 600 nm to 630 nm, but did not extend their work into the yellow, where the current peaks were observed. They also noted that the peaks were degraded towards the red, as are the peaks observed in the present study. A comparison of Howard and Conway’s spectral data to the current data showed some agreement with peaks above 600 nm, but the relative weakness of the peaks made positive identification inconclusive. The evidence suggests, quite plausibly, that the emitter can be identified as molybdenum nitride.


(a) Molybdenum Nitride Deposits on Anode Surface

(b) A Close-up of Molybdenum Nitride Crystals (1000X Magnification)

Figure 5.15: Photographs of Molybdenum Nitride Deposits

5.2.6: H-C_2 Line Ratios

Throughout the spectroscopic studies, attention was focused on the identification of species present within the plasmas and not on the intensity of the spectral lines associated with such species. However, a study of the ratio of line intensities for the H_β and C_2 lines was prompted when the H_β line intensity was observed to exceed the strong C_2 line at 516.5 nm for high currents. For this study, the H_β line and C_2 line at 512.9 nm were chosen, although the ratio of the H_β line to other C_2 lines produced similar trends. A sample methane spectrogram identifying these lines is shown in Figure 5.16a. As shown in Figure 5.16b, the ratio of the H_β line and C_2 band at 512.9 nm increases for higher torch powers. Physically, this indicates the ratio of the concentration of excited hydrogen atoms to diatomic carbon molecules increases as the torch power increases. From the trend line in Figure 5.16b, it appears that the torch power has a linear effect on this ratio. This work could be expanded to heavier hydrocarbons to determine if they also exhibit linear trends. In addition, fuels could be compared to determine whether some fuels produce more hydrogen atoms for a given power input than others. This type of study would then allow the identification of a hydrocarbon feedstock that would provide the most combustion enhancing hydrogen atoms for a given power input.

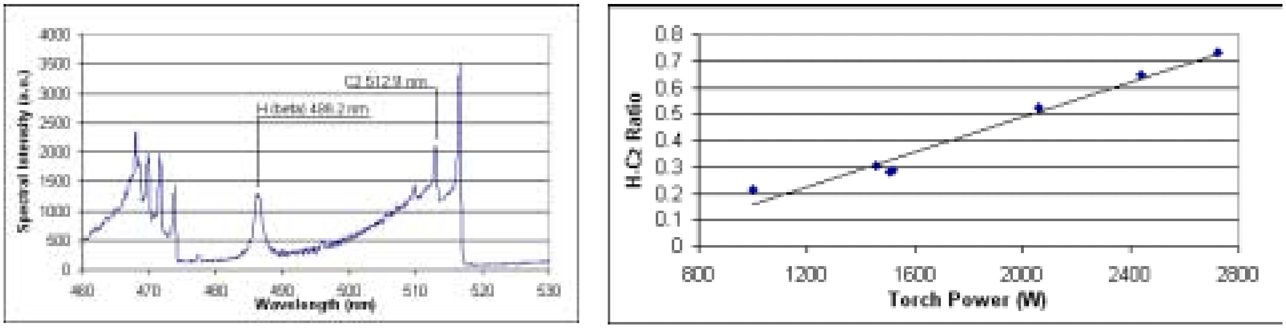

(a) A Reference Methane Spectrogram at 2060 W

(b) H_β-C_2 Ratio versus Power for Methane

Figure 5.16: The Affect of Torch Power on H_β-C_2 Ratio

5.3: Conclusions

This chapter presented the results of spectrographic tests conducted to determine the species present within various hydrocarbon and inert plasmas. The hydrocarbon feedstocks, methane, ethylene, propane and propylene all produced similar spectral signatures, the major species of which are H, C, H_2, C_2, CH, and CH_2. Evidence of plasma-air interaction was detected through the presence of excited CN, NH, CO_2 and N_2. Expectedly, air and nitrogen plasmas produced spectrograms containing an array of oxygen and nitrogen band systems. In addition, two interesting discoveries were made through close observation of the spectrograms produced from the identification studies. One was the observation of the line ratio between the H_β line and C_2. Torch power was shown to have a linear affect on this ratio, demonstrating that plasmas produced at different powers have different concentration ratios. In addition, a discovery was made of new molybdenum nitride peaks, previously unrecorded in the spectroscopic community. These peaks were attributed to the erosion rate of the molybdenum anode and led to the discovery that active nitrogen is particularly erosive to molybdenum. The identification of species present within the plasmas, the observation that the power affects the relative concentration of species in the plasma jet, and the development of an anode erosion detection method, are all scientifically important and form the groundwork on which the material to be presented in following sections is based.